An analysis of $h \to \mu^+\mu^-$ mode at the center-of-mass energy of 500 GeV ILC — part 3

Shin-ichi Kawada

Abstract

[1] This note summarizes the results of $h \to \mu^+\mu^-$ mode at the 500 GeV ILC. This is the third series of note [1, 2]. Here we will discuss more background suppression.

[1]Release note

- 2016/11/8 release
- 2016/11/10 add comment

1 Introduction

In the previous analysis [2], about 20 signals and 120 backgrounds were remained. When I checked the details, most dominant backgrounds were 4f processes, especially the final state of $\nu\nu\mu\mu$ and $\nu\nu\tau\tau$. I tried to work to suppress more these kind of backgrounds.

In the analysis, I used same numbers like cross section, integrated luminosity, and MC samples in ref [2].

2 Analysis using fully-simulated samples

Here I will discuss the analysis with using fully-simulated samples.

2.1 Event reconstruction

The procedure of muon reconstruction is same as written in ref [2].

2.2 Analysis

Before optimization, I required following conditions.

- exactly one μ^+ and one μ^-
- number of tracks which have P_t greater than 5 GeV ($N^{\mathrm{track}}_{P_t>5\mathrm{GeV}}$) should be less or equal to 4
- $124 < M^{\mathrm{FSR}}_{\mu\mu} < 126$ GeV (including FSR correction)
- $\sigma(M_{\mu\mu}) < 1$ GeV

I applied the very last cut as the new precuts. This requires that events should have very well-measured muons, and we will only use this kind of events. The following 4 figures are the distributions of each variable.

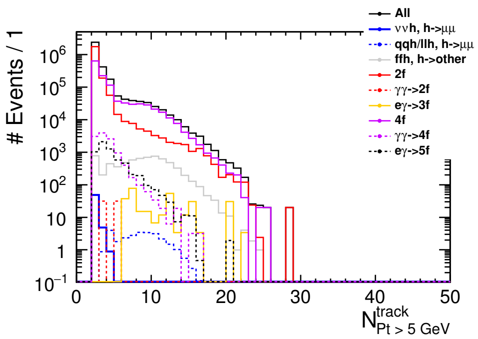

Figure 1: Distribution of $N^{\mathrm{track}}_{P_t>5\mathrm{GeV}}$.

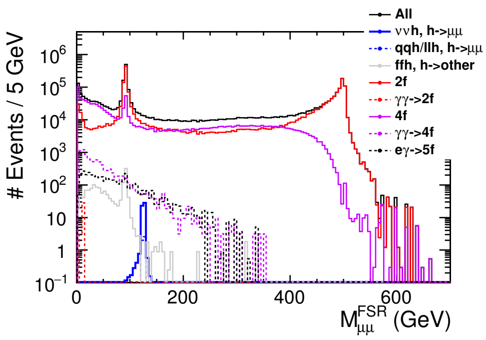

Figure 2: Distribution of $M^{\mathrm{FSR}}_{\mu\mu}$.

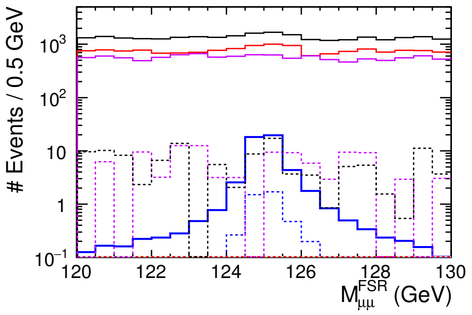

Figure 3: Distribution of $M_{\mu\mu}^{\text{FSR}}$ (zoomup).

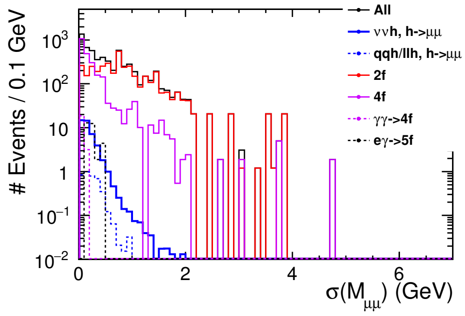

Figure 4: Distirbution of $\sigma(M_{\mu\mu})$.

The 3f processes are completely eliminated at this stage. After these, I required following cuts as the optimum.

- visible energy $E_{\text{vis}} < 270$ GeV
- $P_t > 45$ GeV
- (charge) $\times(\cos\theta_{\mu^+}^{\text{FSR}}) > -0.75$ and (charge) $\times(\cos\theta_{\mu^-}^{\text{FSR}}) > -0.75$
- thrust < 0.88
- $E_{\mu^+\mu^-} > 160$ GeV

where P_t is computed transverse momentum from the four-momentum of summing up of all visible particle's four-momentum. The third variable is flight direction of particle multiplied by its charge. The $WW \to \mu\nu\mu\nu$ backgrounds are tend to distribute around $+1$ or -1 (-1 in this study), but signal does not have such kind of feature. This variable is useful to characterize the event which opposite signed charged particles flight to each other in opposite direction. The following 6 figures are the distributions of each variable.

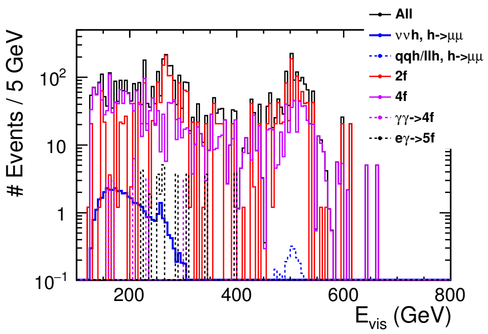

Figure 5: Distribution of E_{vis}.

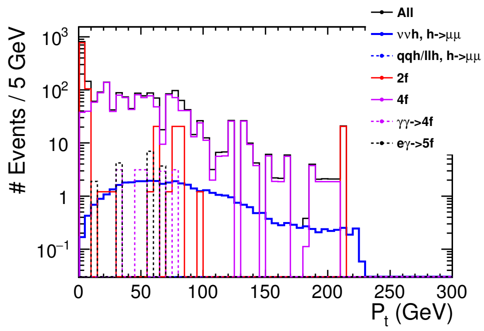

Figure 6: Distribution of P_t.

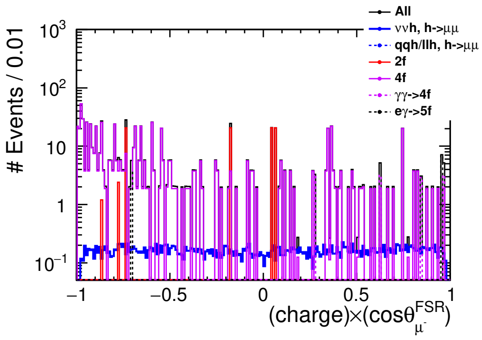

Figure 7: Distribution of (charge) $\times(\cos\theta^{\mathrm{FSR}}_{\mu^-})$.

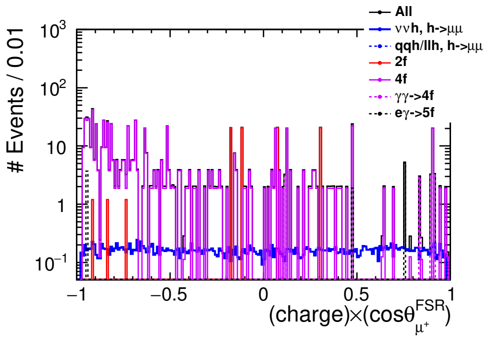

Figure 8: Distribution of (charge) $\times(\cos\theta^{\mathrm{FSR}}_{\mu^+})$.

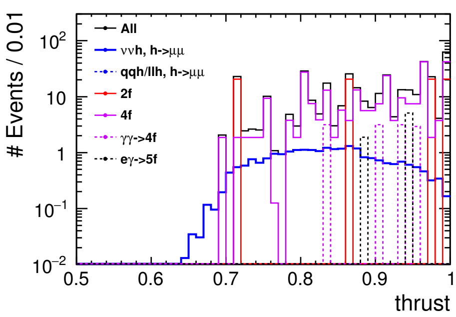

Figure 9: Distribution of thrust.

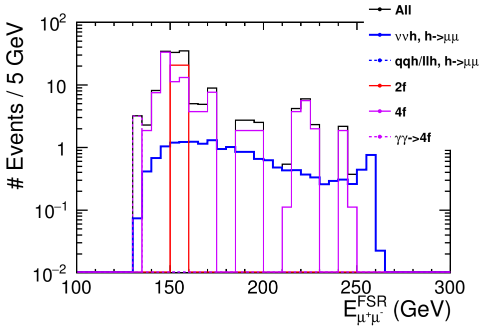

Figure 10: Distribution of $E_{\mu^+\mu^-}$.

Table 1 shows the cut table using fully-simulated samples.

Table 1: Cut table using fully-simulated samples.

	$\nu\nu h$ $h\to\mu\mu$	$qqh+\ell\ell h$ $h\to\mu\mu$	ffh $h\to$ other	2f	$\gamma\gamma\to$ 2f	3f	4f	$\gamma\gamma\to$ 4f	5f
No cut	57.53	31.13	4.116×10^5	4.224×10^7	4.283×10^9	4.269×10^8	4.592×10^7	3.356×10^5	2.209×10^5
# $\mu^\pm$	54.39	27.39	6895.00	2.071×10^6	62.62	299.75	1.209×10^6	1.131×10^4	6125.00
# $N^{\mathrm{track}}_{P_t>5\mathrm{GeV}}$	54.27	4.89	1425.76	2.014×10^6	31.28	0	9.826×10^5	9544.48	4411.00
$M^{\mathrm{FSR}}_{\mu\mu}$	44.61	3.94	0	3741.41	0	0	2407.24	21.81	31.63
$\sigma(M_{\mu\mu})$	44.28	3.92	0	2619.66	0	0	2295.69	21.81	31.63
E_{vis}	41.38	0.04	0	966.60	0	0	1273.28	15.52	16.74
P_t	31.55	0.02	0	86.00	0	0	676.33	12.37	10.64
charge $\times\cos\theta_\mu$	24.42	0.01	0	82.39	0	0	261.77	12.37	6.96
thrust	17.67	0.01	0	41.19	0	0	101.15	3.15	0
$E_{\mu\mu}$	13.04	0.01	0	0	0	0	34.20	0	0

From this analysis, I obtained $N_{\mathrm{sig}} = 13.04$ and $N_{\mathrm{bkg}} = 34.21$. The signal significance was calculated to be $\frac{13.04}{\sqrt{13.04+34.21}} = 1.90$ and its corresponding precision was $\frac{\Delta(\sigma\times\mathrm{BR})}{(\sigma\times\mathrm{BR})} = 53\%$. This result is improved slightly than previous, but the final precision number is almost same.

3 For further improvement

We have following ideas for the improvement.

- event-by-event reweighting using $\sigma(M_{\mu\mu})$, and its statistical interpretation

- better efficiency for muon reconstruction
- use TMVA
- categorizing

First: ignore because I still don't understand. Second: try to do more efficient muon reconstruction. Third: move to multivariate analysis. Fourth: separate Higgs-strahlung category and WW-fusion category, and optimize each category. In this note, we will discuss second and third.

4 Muon reconstruction

Here we will consider muon reconstruction again. The muon reconstruction method previously used are following.

- select muon candidate
  - charge
  - energy
  - $E_{\rm ECAL}/(E_{\rm ECAL} + E_{\rm HCAL})$
  - $(E_{\rm ECAL} + E_{\rm HCAL})/|p_{\rm track}|$
- FSR recovery
  - find neutral particles flighting very near angle with respect to reconstructed muon
  - summing up four-momentum of selected neutral particles
- events which have opposite muons, and muon pair invariant mass including FSR correction with the range between 124 GeV and 126 GeV

I think there should be some rooms for improvement in muon selection and FSR recovery. In this note we will only discuss muon reconstruction.

4.1 Muon selection

In order to select muons, it is important to use the information of energy deposit in calorimeter and the momentum of track. The following 2 figures show the distribution of $E_{\rm ECAL}/(E_{\rm ECAL} + E_{\rm HCAL})$ and $(E_{\rm ECAL} + E_{\rm HCAL})/|p_{\rm track}|$.

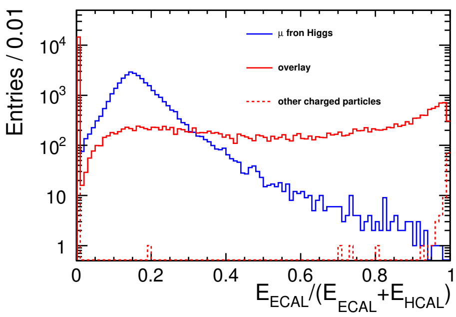

Figure 11: Distribution of $E_{\rm ECAL}/(E_{\rm ECAL} + E_{\rm HCAL})$.

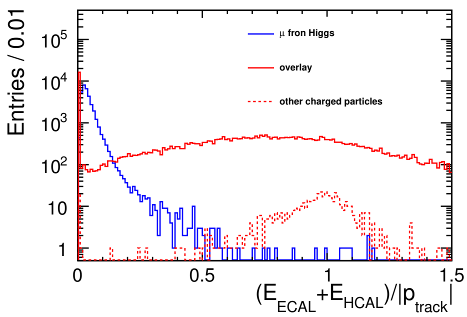

Figure 12: Distribution of $(E_{\rm ECAL} + E_{\rm HCAL})/|p_{\rm track}|$.

The "Other charged particles" were almost electrons and positrons. These particles might be generated due to detector interaction. As we can see, the problematic particles are overlay particles. At this stage, I want to have good efficiency, I can loosen the cuts for these variables. Of course many overlay particles will survive, we will consider next. I defined muon selection cut from these 2 figures as following.

- $E_{\mathrm{ECAL}}/(E_{\mathrm{ECAL}}+E_{\mathrm{HCAL}}) < 0.95$
- $(E_{\mathrm{ECAL}}+E_{\mathrm{HCAL}})/|P_{\mathrm{track}}| < 0.5$

Next, I tried to reduce the contamination of overlay particles. The P_t would be the best variable. Furthermore, the energy deposit in yoke E_{yoke} also would be useful. The following 2 figures are the distributions of P_t and E_{yoke} after the cuts of muon selection.

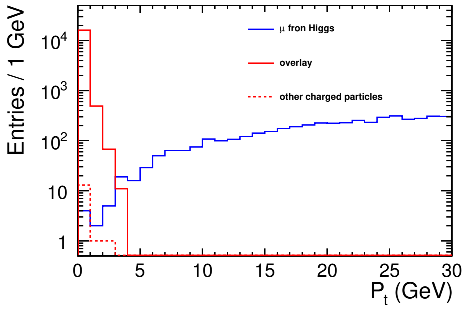

Figure 13: Distribution of P_t (after muon selection cut).

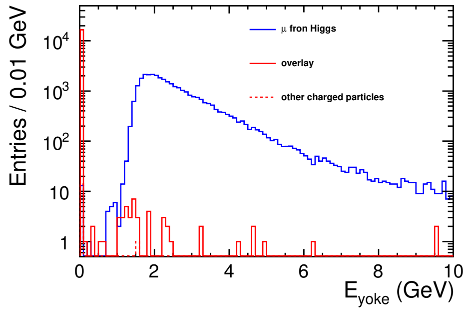

Figure 14: Distribution of E_{yoke} (after muon selection cut).

I defined the following cuts.

- $P_t > 3$ GeV
- $E_{\mathrm{yoke}} > 1$ GeV

The purity in the signal sample was almost 100%. At this point, the reconstruction efficiency was 96.3% (defined as number of signal events with exactly reconstructed one μ^+ and one μ^- divided by total signal events). The previous efficiency was 94.6%. This is the improvement by relatively 2%. In the remaining 3.7% events, the muons flight to beam direction or very near to 90°, we cannot get any information of them.

4.2 Precuts

Previously I required the invariant mass range with FSR correction between 124 GeV to 126 GeV. However this cut is already very tight and I will use TMVA furthermore, I decided to loose this range. In addition, I took a policy to select only very well-measured muons using track information. Under this policy, I applied following cuts.

- exactly one μ^+ and one μ^-
- $\sigma(M_{\mu\mu}) < 1$ GeV
- $\chi^2/\mathrm{Ndf}(\mu^\pm) < 2$
- innermost hit $(\mu^\pm) < 100$ mm
- $30 < M_{\mu\mu} < 130$ GeV
- $125 < E_{\mathrm{vis}} < 400$ GeV

Second cut is requiring only very well-measured muon pair, and its distribution is shown in the following figure.

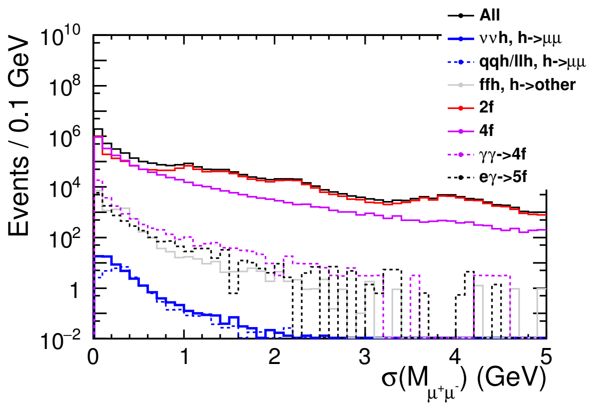

Figure 15: Distribution of $\sigma(M_{\mu\mu})$.

Third cut is relevant to track fitting parameter. If this value is very small, that means the track is well fitted. Fourth cut is requiring where is the first track hit in the detector. This cut is applied for both μ^+ and μ^-. The remaining two loose cuts are used to determine signal region. Since the training time in TMVA will increase when the number of events are huge, it is important to apply cuts (even loose). It is important to apply even loose cuts because the training time will increase when the number of events are increased. The following figures are the distributions of each variable.

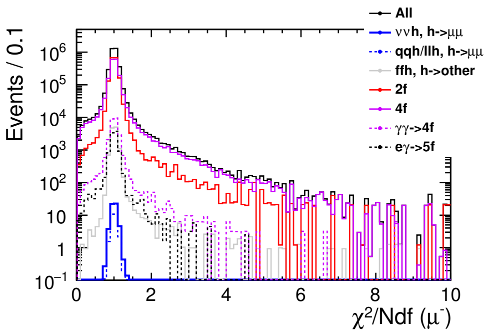

Figure 16: Distribution of $\chi^2/\mathrm{Ndf}(\mu^-)$.

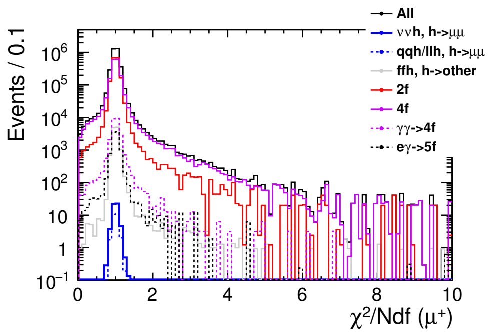

Figure 17: Distribution of $\chi^2/\mathrm{Ndf}(\mu^+)$.

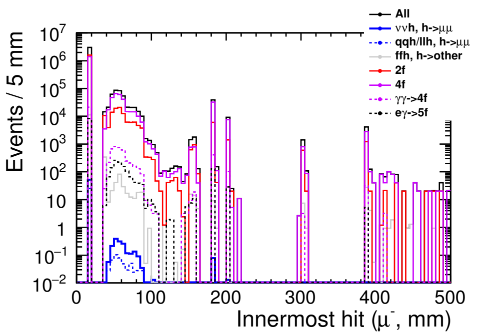

Figure 18: Distribution of μ^- innermost hit.

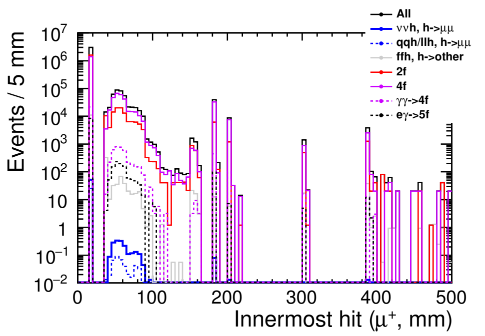

Figure 19: Distribution of μ^+ innermost hit.

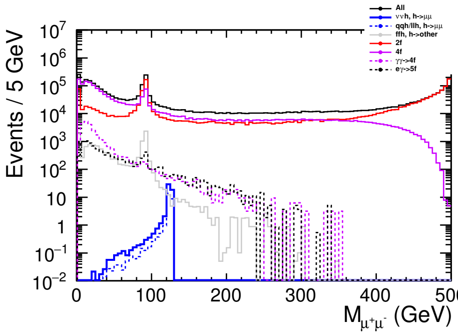

Figure 20: Distribution of $M_{\mu\mu}$.

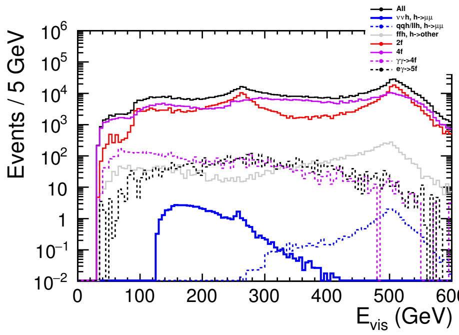

Figure 21: Distribution of E_{vis}.

Table 2 shows the cut table at the precuts. The 3f and $\gamma\gamma \to 2\text{f}$ which is SGV sample are not included because SGV sample cannot handle energy deposit in yoke properly.

Table 2: The cut table using fully-simulated samples.

	$\nu\nu h$ $h \to \mu\mu$	qqh+$\ell\ell h$ $h \to \mu\mu$	ffh $h \to$ other	2f	4f	$\gamma\gamma \to$ 4f	5f
No cut	57.53	31.13	4.116×10^5	4.224×10^7	4.592×10^7	3.356×10^5	2.209×10^5
# $\mu^\pm$	55.32	26.12	1.216×10^4	2.246×10^6	1.890×10^6	2.692×10^4	9935
$\sigma(M_{\mu\mu})$	54.60	25.64	1.202×10^4	1.728×10^6	1.785×10^6	2.638×10^4	9690
χ^2/Ndf	54.52	25.61	1.187×10^4	1.719×10^6	1.753×10^6	2.599×10^4	9573
innermost hit	54.28	25.55	1.163×10^4	1.698×10^6	1.660×10^6	2.481×10^4	9225
$M_{\mu\mu}$	54.24	25.53	6506	4.200×10^5	5.488×10^5	5787	4114
E_{vis}	54.16	2.71	1879	1.948×10^5	2.802×10^5	3419	3225

Backgrounds suppressed 2 order of magnitude while remaining signals.

4.3 TMVA analysis

I used TMVA BDTG for the analysis. I used following 14 parameters.

- E_{vis}、P_t、thrust、$\cos\theta_{\text{thrust}}$、$\cos\theta_{\text{miss}}$
- $M_{\mu\mu}$、$E_{\mu\mu}$、$P_{t,\mu\mu}$、$\cos\theta_{\mu\mu}$、$p_{\mu\mu}$
- charge * $\cos\theta_{\mu^+}$、charge * $\cos\theta_{\mu^-}$、leading energy of muon、subleading energy of muon

I optimized each training parameter. The following figures show the distribution of each input variable.

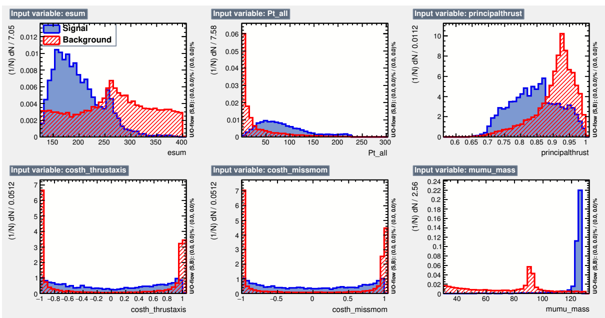

Figure 22: Parameter distribution 1.

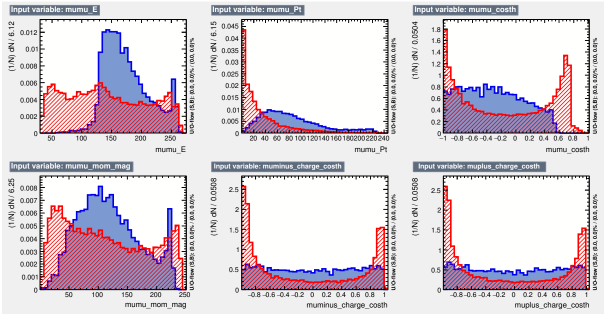

Figure 23: Parameter distribution 2.

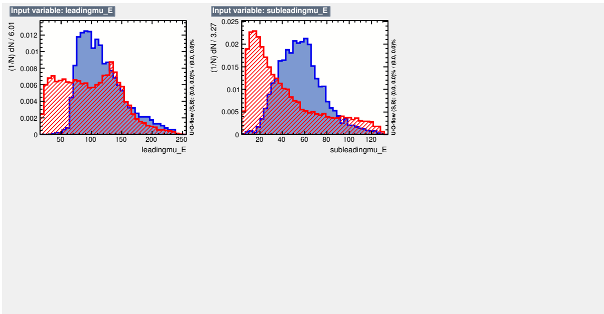

Figure 24: Parameter distribution 3.

The following 2 figures show the results of TMVA analysis.

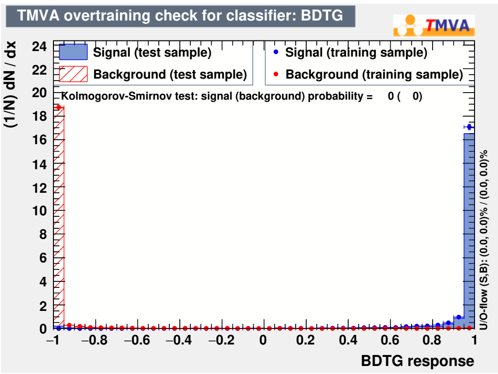

Figure 25: Distribution of BDTG output.

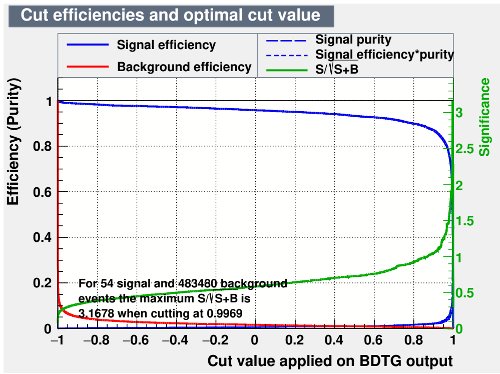

Figure 26: Distribution of significance.

From this analysis, I obtained $N_{\mathrm{sig}} = 24.2$ and $N_{\mathrm{bkg}} = 34.3$. The signal significance was calculated to be 3.16, this corresponds to the precision of $\dfrac{\Delta(\sigma \times \mathrm{BR})}{(\sigma \times \mathrm{BR})} = 32\%$. This result is improved by factor 2. But unfortunately, we can clearly see the overtraining. So it is dangerous to believe these numbers only. At least I am going to good direction, but more careful study is needed.

5 Summary

I re-visited the analysis for the improvement. With using TMVA, the precision improved to 32%, but this is overtrained result. I need more careful study.

For future task, the following things need to be considered.

- FSR correction
- reweighting
- separation between Higgs-strahlung process and WW-fusion process

References

[1] Shin-ichi Kawada "An analysis of $h \to \mu^+\mu^-$ mode at the center-of-mass energy of 500 GeV ILC"

[2] Shin-ichi Kawada "An analysis of $h \to \mu^+\mu^-$ mode at the center-of-mass energy of 500 GeV ILC — part 2"